Journal of Power Sources 183 (2008) 564–570

Contents lists available at ScienceDirect

Journal of Power Sources

journal homepage: www.elsevier.com/locate/jpowsour

Molecular speciation of sulfur in solid oxide fuel cell anodes with X-ray absorption spectroscopy

Artur Braun[a,*], Markus Janousch[b], Josef Sfeir[c], Jari Kiviaho[d], Matti Noponen[d], Frank E. Huggins[e], Martin J. Smith[f], Robert Steinberger-Wilckens[f], Peter Holtappels[a], Thomas Graule[a]

[a] *Laboratory for High Performance Ceramics, Empa-Swiss Federal Laboratories for Materials Testing & Research, CH-8600 Dübendorf, Switzerland*
[b] *Swiss Light Source, Paul Scherrer Institut, CH-5232 Villigen PSI, Switzerland*
[c] *HEXIS AG, CH-8404 Winterthur, Switzerland*
[d] *VTT Technical Research Centre of Finland, FIN-02044 Espoo, Finland*
[e] *Department of Chemical and Materials Engineering, and Consortium for Fossil Fuel Science, University of Kentucky, Lexington, KY 40506, USA*
[f] *Institute for Materials and Processing of Energy Systems, Forschungszentrum Jülich, D-52425 Jülich, Germany*

ARTICLE INFO

Article history:
Received 21 February 2008
Received in revised form 25 April 2008
Accepted 3 May 2008
Available online 23 May 2008

Keywords:
SOFC
Sulfur
Sulphur
Anode
Poisoning
Molecular speciation
Thiophene
X-ray absorption
Spectroscopy
XANES

ABSTRACT

Two sets of solid oxide fuel cell (SOFC) electrode assemblies from different manufacturers were run under different operating conditions with different sulfur exposure, and then subjected to X-ray absorption spectroscopy (XAS) at the sulfur K (1s) edge. Within the detection limits of the spectrometer, pristine fuel electrodes (anodes) show no traces of sulfur. The anodes operated with sulfur-containing natural gas and H_2S doped natural gas show spectra rich in sulfur structures. Two other electrodes run with sulfur-containing natural gas, one with a sulfur filter and the other without, show an XAS spectrum with a very broad peak, covering the entire sulfur absorption range, and thus not allowing for identification of specific sulfur signatures. These appear to be the first ever reported sulfur XAS data on SOFC anodes, and the XAS technique shows promise to resolve some hitherto unsolved issues on sulfur poisoning of SOFC, particularly regarding the molecular speciation of the sulfur components.

1. Introduction

Solid oxide fuel cells (SOFC) have a high potential of becoming an important and environmentally benign electrochemical energy conversion device [1]. The fuel electrodes (anodes) of SOFC are in their majority made from nickel and yttria stabilized zirconia (YSZ). From Ni and YSZ, a porous metal–ceramic (cermet) with thicknesses ranging from 100 to 1000 μm is produced (substrate) on which the actual anode of the same material, but with a modified microstructure is applied in a thickness of 10–20 μm (anode-supported cell, ASC). Alternatively, a thin anode layer (50 μm) can be deposited on a YSZ electrolyte support structure of around 100-μm thickness (electrolyte supported cell, ESC). "Sulfur poisoning" refers to the malign chemical reaction of trace sulfurous gases present in fuels, with the nickel catalyst present in many anodes. As a result of the reaction with sulfur, the anode catalyst is deactivated, degrades and ultimately deteriorates to uselessness [2]. This issue has been increasingly addressed recently [3–5], but technical solutions to prevent or mitigate poisoning remain to be proven. The chemical composition of the sulfur species is not yet known, despite extensive and fruitful research on Ni–S chemistry in petrochemical industry catalysis [6].

Spectroscopy techniques have increasingly been used for chemical analysis. In SOFC studies, optical Raman spectroscopy has been applied, see for instance [7], but vibration spectroscopy including infrared spectroscopy is not specific to any element, particularly not to sulfur. In addition, these techniques are insensitive to Raman inactive and infrared inactive molecules. Furthermore, the Raman effect is a rare event from a statistical point of view and hence requires high sulfur concentrations. X-ray photoelectron spectroscopy has also been used [8], but this is a pronounced surface

* Corresponding author. Tel.: +41 44 823 4850; fax: +41 44 823 4150.
E-mail address: artur.braun@alumni.ethz.ch (A. Braun).

0378-7753/$ – see front matter © 2008 Elsevier B.V. All rights reserved.
doi:10.1016/j.jpowsour.2008.05.048

sensitive technique and results are not necessarily representative of the entire anode.

It is quite surprising that sulfur XAS has never been reported with respect to SOFCs, although sulfur K-edge XAS is chemically specific to sulfur. The K-shell X-ray absorption edge of sulfur is located at around 2470 eV and thus permits a sampling depth of several microns for a typical porous anode assembly.

XAS has been applied in energy materials science and technology particularly often with respect to transition metals in catalysis ([6] and references therein), or transition metals and alkaline metals in batteries [9,10] and fuel cells [11], for carbon [12] and sulfur in fossil fuels [13–15], battery [16] or metallurgical engineering [17], some of them being more recent novelties. Sulfur XAS can now be considered a mature technique for chemical analysis. To the best of our knowledge, our work is the first application of sulfur XAS in SOFC research.

2. Experimental

The first set of samples was manufactured according to industrial standards by HEXIS AG, Switzerland. A composite cathode made of lanthanum strontium manganite (LSM) and YSZ, and an anode cermet composed of nickel and cerium gadolinium oxide (Ni/CGO) of 35-μm thickness each were screen printed on a 140-μm thick 3YSZ electrolyte (3% yttria) manufactured by Nippon Shokubai Co. Ltd., Japan. The cells were then sintered at temperatures above 1000 °C. Electrochemical tests were made on short stacks of five cells sandwiched between metallic interconnectors provided by Plansee SE, Austria. The cells were run at 950 °C using natural gas reformed in a catalytic partial oxidation reactor (CPO) with a fuel/air-mixing ratio of $\lambda \approx 0.27$.

Sample A is the pristine electrode coming out of the assembly line, with no further treatment or operation. Sample B was employed for 1000 h at 950 °C in an SOFC short stack, fueled with natural gas containing 7 ppm tetrahydrothiophene (THT). The stack was shut down by closing the fuel supply. Sample C was run-like B, but equipped with a sulfur filter.

The second set of samples was manufactured according to Forschungszentrum Jülich (Research Centre, Jülich) standard specifications [18], i.e. using a 1500-μm thick NiO/8YSZ anode substrate, a 10 μm NiO/8YSZ anode functional layer, a 10-μm thick 8YSZ electrolyte layer, and a 70-μm thick LSM/YSZ cathode layer. These samples were set up at VTT Finland in three different SOFC single cell tests, #40 run with pure hydrogen, #46 run with natural gas reformats containing 6 mol ppm thiophene, and #49 run with natural gas reformats containing 6 mol ppm thiophene plus 1 mol ppm H_2S. The tests were run for 200 h each at 800 °C and then shut down in an atmosphere containing 5 mol% H_2, 3 mol% H_2O and 92 mol% N_2. Prior to entering the anode, the fuel passes an autothermal reactor (ATR) so that the resultant fuel gas is made up of hydrogen, carbon monoxide, thiophene, water, oxygen and nitrogen, and then through a ZnO bed for desulfurization. Since the ATR ZnO bed was operated in excess of 5000 h, we cannot entirely rule out that it might have been saturated with sulfur, and that it might have released thiophene [18].

From the aforementioned electrodes run in the tests, pieces of 5 mm × 5 mm size were cut out after SOFC operation and then subjected to S K-edge XAS spectroscopy at the LUCIA beamline at the Swiss Light Source [19]. Spectra were recorded in a light vacuum of $p \approx 5E{-}4$ Torr in the fluorescence mode with a defocussed beam at 0.2 eV energy resolution and 30 min data acquisition time per scan. For every sample, five scans were recorded ranging from 2400 to 2650 eV.

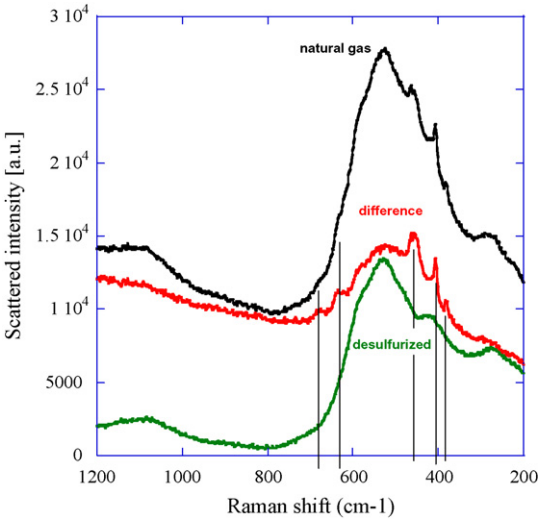

Fig. 1. Optical Raman spectra of cells from stack C (black spectrum, top) and B (bottom, green), which was run with a sulfur filter. The red spectrum in the middle was obtained by forming the difference of spectra C minus B: $I_C - I_B$.

3. Results and Discussion

Prior to presenting the X-ray absorption data, we want to briefly show a set of optical Raman spectra. Fig. 1 shows the Raman spectra of a sulfur-free (run with desulfurized gas) and a sulfur-exposed SOFC sample (run with sulfur-containing natural gas). Subtracting the spectrum of sulfur-free sample from the sulfur-exposed spectrum should yield a spectrum, which specifically highlights the sulfur-specific characteristics of the spectrum, and so the sample. This difference spectrum then should basically allow for identification of species that are related to sulfur exposure. We notice distinct features at 670, 630, 454, 440, 406 and 381 wavenumbers (1 cm^{-1}). The band at 454 (1 cm^{-1}) is close to 480 and 470 (1 cm^{-1}), which have been previously assigned to NiS_2 or FeS_2, respectively. The band at 406 is close to 400 (1 cm^{-1}) which is known to be a genuine S–S stretching mode. The feature at 381 (1 cm^{-1}) can be assigned to Ni_3S_2 and FeS_2, which have bands at 361 and 381, respectively. Our assignments are based on reference data published in Refs. [20–23] and summarized in Table 1. Further discussion of the Raman spectra, particularly with respect to the question whether or to what extent Fe or Cr species may be present in our samples, for instance as impurities, is beyond the scope of this manuscript. What becomes clear is that an element-specific characterization technique is desirable.

The sulfur K-shell absorption spectra from specimens #46 and #49 (FZ Jülich Research Center) are rich in sulfur-specific signatures, as shown in Fig. 2. For the peak assignment and deconvolution of the spectra, we refer to previously published reference data [13,14,17]. The spectra look virtually identical. The strongest peak is at 2482.2 eV and can be assigned to sulfate. The next strongest peak is at 2473.5 eV and assigned to a generic thiophene structure, which furtheron will be referred to simply as thiophene. Incidentally, there is likely a range of polycyclic S-heterocyclic compounds found in natural gas as well as the monocyclic thio parent. The immediate sulfur chemical environment may be quite similar in all cases, and since few reference spectra on different thiophene moieties are available, one cannot tell from the data available here which particular thiophenic species may actually be present. For example, there is a wealth of NEXAFS literature on the large complex of organic carbon species [12,24], but a similar compendium that would allow for assignment of specific organic sulfur compounds has yet to be developed.

Table 1
Raman signatures for reference materials

Species	peak [cm^{-1}]																				
measured	**670**	**630**				**454**	**440**	**406**	**381**												
Ni_3S_2									**361**		**324**	**305**				223			201	190	
							438							**272**		**226**	218	211		185	
Ni_7S_6																					
NiS									**369**	**349**		**300**	283		**244**						144
β-NiS									372	350		301	283		246	222				181	
α-NiS										344			286		238	222				181	
Ni_3S_4									382	337			**288**			224		208			
NiS_2					515		468		414					274	235						
						490	**480**						285	274							
FeS_2							**470**			**381**											
S-S bond								**400**													
Cr_2O_3	656	619	568				443	412				305									
		609	551	530				397		351		303									
Fe_2O_3 hematite		613			497			411				301	292		245	226					
NiO				525																	
YSZ		600																			

Reference data taken from Refs. [8,20–23].

The other, less strong resonances are from sulfone at 2480.5 eV, elemental sulfur at 2472.4 eV, and sulfide at 2472 eV. Sulfoxide and sulfones are mono-/polycyclic S-heterocycle partial oxidation products. Possibly they arise from poly heterocycles rather than thiophene itself. The positioning of the arctangent function for the deconvolution of the spectra is critical here and may lead to some ambiguity in the peak-fitting approach. Hence we believe we possibly have a mixture of different heterocycles, such as di- and tri-benzo variants. Within the systematic uncertainties just mentioned, the peaks due to the different sulfur functionalities can be unambiguously assigned and easily deconvoluted. The application of two-step functions (arcus tangens) for the ionization potential, as exercised in Fig. 2, is not commonly necessarily for XAS, but has proven advantageous and is generally accepted for analysis of sulfur XAS spectra.

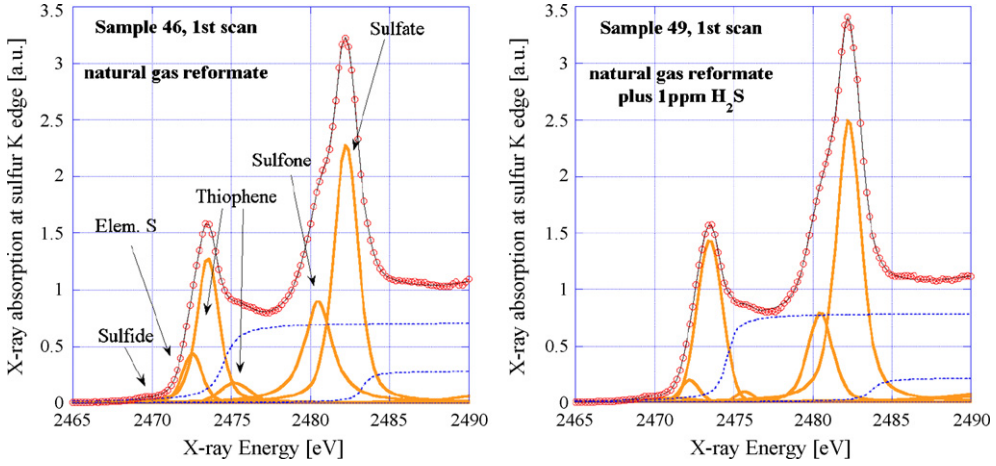

Fig. 2. Sulfur XAS spectra from anodes from FZ Jülich fuelled with thiophene-containing natural gas (sample #46), and with such natural gas plus H_2S added (sample #49).

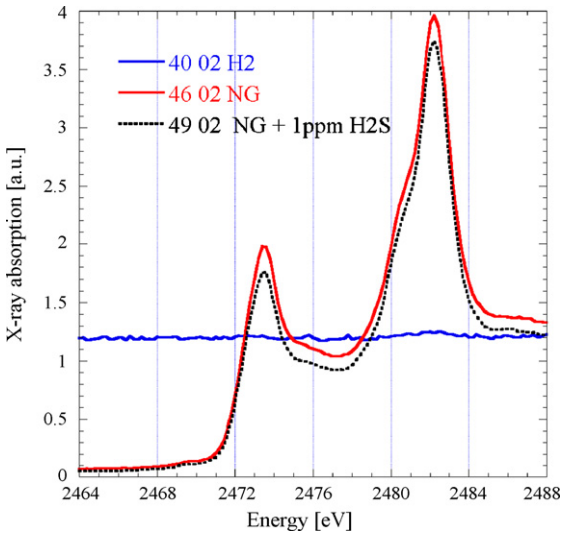

Fig. 3. Comparison of the spectra of the three FZ Jülich samples #40, #46, and #49.

Although the proximity of the sulfur and thiophene peaks might suggest that thiophene could be mistaken for elemental sulfur, the peak positions as well as the peak distances, such as between thiophene and sulfate, serve as an additional internal spectral reference, which confirm that the peak at 2473.6 eV is to be attributed to thiophene. Many other authors have shown the presence of both components in a wide variety of substances, especially in environmental studies.

In order to test whether the reference sample #40, not intentionally exposed to sulfur, would exhibit any sulfur from exposure to ambient conditions, we measured this sample as well. Within the detection limit of the spectrometer, no trace of sulfur could be made out on sample #40 (see Fig. 3). Therefore the spectra of samples #46 and #49 represent the sulfur in the anode after operation of the cell with sulfur-containing fuel.

The fact that we identify thiophene in the samples is surprising and has stimulated some debate among the co-authors of this work. The thiophene that is included in the natural gas should have been decomposed at 800 °C, and the resulting H_2S should have been captured in the ZnO bed at 400 °C. However, thiophene may also have desorbed from internal gas pipe surfaces or from the autothermal reactor during the final stages of cooling. We also need to point out that the concentration of sulfur in the anodes is as low as some 10 mol ppm only. One cannot rule out that very small amounts of thiophene may survive the high temperatures. Thiophene has also been detected in unburnt carbon in coal fly-ash from coal burning power plants with temperatures in excess of 1200 °C [13,14].

Note that all spectra shown here were recorded when the sample was at ambient temperature, whereas the sulfur species may have reacted with the anode material at temperatures as high as 800 °C. The species grown at 800 °C may transform to what we find at ambient temperature during the cooling process. Although the source of the thiophene cannot be completely explained here, the fact that this signal is found points to potential shortcomings of post-operational analysis in SOFC. When analyzing cell components, care has to be taken to preserve the conditions that were present during operation for the analysis process. This implies close and careful control of gas compositions during the cool down process. Nevertheless, as just stated, reactions taking place during the cooling to room temperature can obliterate the findings. A case can be made here for high-temperature and in situ XAS that would avoid the cooling process and limit subsequent creation of artefacts.

Fig. 4 shows a sequence of repeated scans for both samples #46 and #49. We notice a small sulfide peak, and a decrease of the sulfate peak with respect to the thiophene peak. This kind of systematic peak height rearrangement is not uncommon and possibly due to "radiation damage" [25,26]: the synchrotron beam dissipates energy and transforms to thermal energy on the sample, potentially altering the sample chemistry and composition. The observed peak height variation upon scanning thus suggests that at high temperatures the sulfate peak is smaller, whereas the thiophene peak is larger. Table 2 summarizes our peak assignments and fitting parameters. The evolution of the relative peak heights for sulfate and thiophene for the six scans is plotted in Fig. 5. Sulfide, sulfur and thiophene are increasing upon continuing irradiation, whereas sulfone and sulfate are decreasing. From the evolution of the relative peak heights of all species we can conclude, however, that the spectra after the first few scans are approaching equilibrium. An alternative interpretation is that these changes could be the result of doing the experiment in a partial vacuum. Certain sulfur species could be reduced or be devolatilized as a result of heating due to the beam in the partial vacuum. Such changes are not seen in successive scans of a fossil fuel (for example) in a helium-filled sample arrangement.

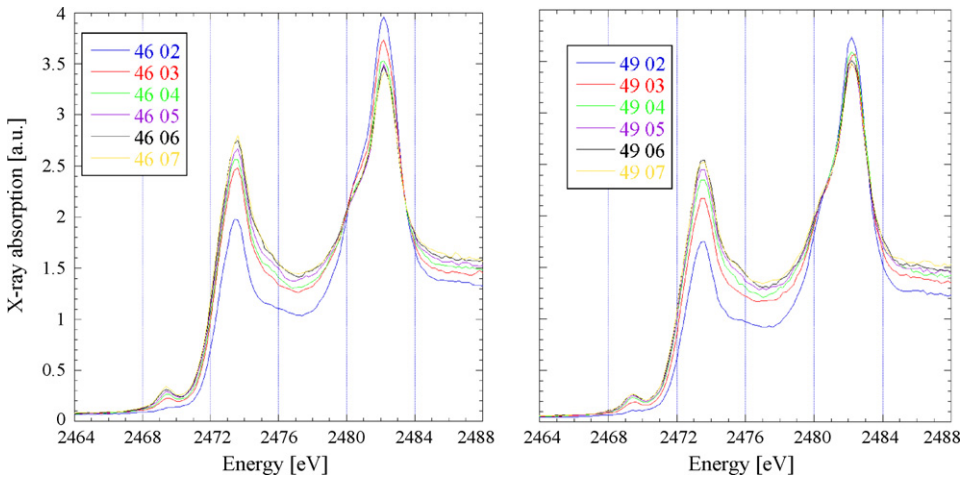

Fig. 4. Sequence of scans for the two FZ Jülich SOFC anodes with sulfur signature, #46 and #49.

Table 2
Fitting parameters for the scans of sample #49 from FZ Jülich

Label	Sulfide	El. Sulfur	Thiophene	Thiophene	Sulfone	Sulfate
	Height	Height	Height	Height	Height	Height
	Pos'n, eV	Pos'n, eV	Pos'n, eV	Pos'n, eV	Pos'n, eV	Pos'n, eV
	Width, eV	Width, eV	Width, eV	Width, eV	Width, eV	Width, eV
# 49_02	0.07	0.31	1.38	0.15	0.94	2.44
	2471.55	2472.35	2473.52	2475.54	2480.52	2482.27
	4.1	1.4	1.7	1.8	2.0	1.8
#49_03	0.08	0.60	1.55	0.17	0.56	2.02
	2469.41	2472.48	2473.61	2475.56	2480.39	2482.28
	1.1	1.7	1.8	2.2	2.0	2.1
#49_04	0.12	0.71	1.68	0.24	0.63	1.92
	2469.42	2472.40	2473.60	2475.42	2480.48	2482.30
	1.0	1.7	1.8	2.0	2.6	2.0
#49_05	0.13	0.66	1.73	0.33	0.55	1.83
	2469.42	2472.33	2473.58	2475.42	2480.48	2482.29
	1.1	1.8	1.8	2.5	2.7	2.0
#49_06	0.14	0.79	1.80	0.32	0.46	1.89
	2469.37	2472.35	2473.62	2475.56	2480.40	2482.25
	1.1	1.8	1.8	1.8	2.6	2.1
#49_07	0.14	0.80	1.70	0.33	0.55	1.77
	2469.38	2472.37	2473.57	2475.45	2480.37	2482.30
	1.2	1.8	1.7	2.2	2.6	2.0

The second set of samples (HEXIS AG) shows an entirely different picture. Fig. 6 displays the spectra of the three samples A, B, and C. The only sample whose spectrum shows a sulfur-specific signal is the one operated without the sulfur filter, sample C. We recall that the fuel was natural gas containing 7 ppm THT as provided by the local gas supplier. The spectrum shows a very broad intensity from 2460 to 2490 eV, which hardly can be called "peak". A particular peak assignment is not justified, given the broad convolution of features, and we have not attempted any deconvolution of the spectrum. Since the onset of this feature occurs at the very low end of the range for sulfur moieties, we cannot rule out that it may represent the onset of a thin amorphous sulfide surface layer being formed on the ceramic.

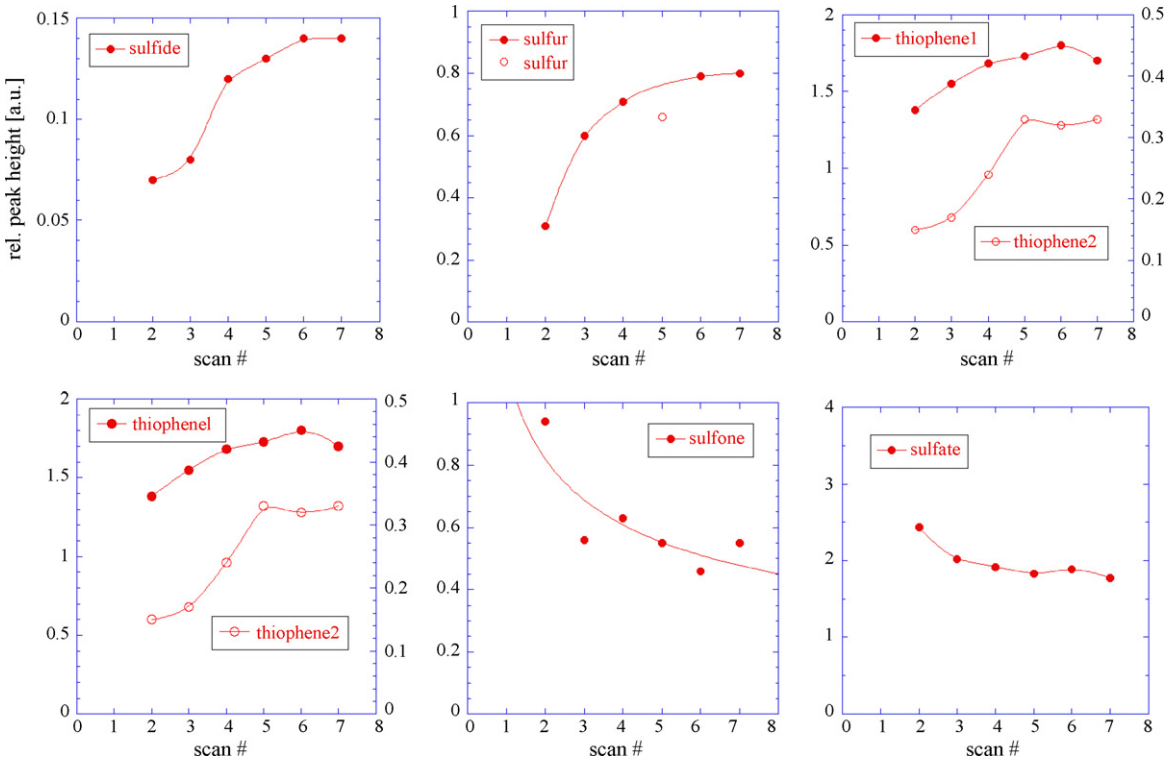

Fig. 5. Evolution of species obtained from XAS fitting parameters for sample #49 (peak height in normalized spectra) plotted vs. the scan sequence. Solid lines merely serve as guide to the eye.

This speculation, and also the request of an anonymous reviewer, point us to the morphology and pore space topology of the anodes. All the samples introduced here have recently been subject to anomalous ultra-small angle X-ray scattering (USAXS) with respect to the Ni K-edge and Zr K-edge at the UNICAT Beamline at the Advanced Photon Source in Argonne National Laboratory, USA. Scattering curves were recorded across the cathode, electrolyte and anode in steps of 10–15 mm and allow for the resolution of objects with sizes from 1 nm to roughly 1000 nm. The analysis of the USAXS data is not yet finished, but preliminary evaluation indicates that a 500 nm large primary mode in the pristine anode decreases to around 200 nm upon operation with and without sulfur in the fuel.

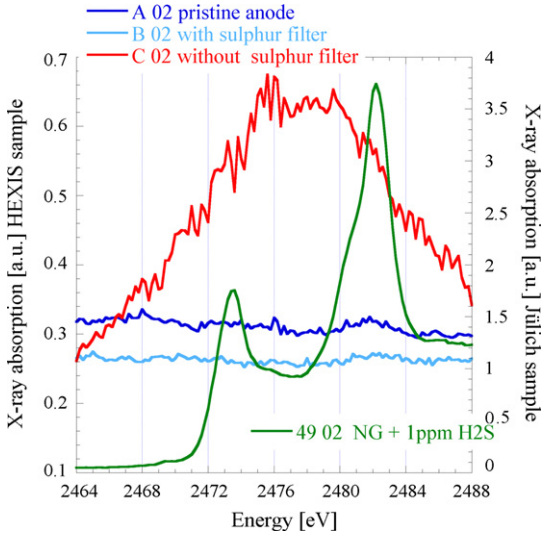

Fig. 6. Comparison of the three HEXIS samples (flat blue spectra and red broad spectrum). One FZ Jülich spectrum from sample #49 is shown for comparison.

At this time we cannot further comment on the structural changes on any scale of these samples, but we will treat this topic in a separate work [28].

4. Conclusions

X-ray absorption spectroscopy at the sulfur K-edge is capable of determining the molecular speciation of sulfur moieties in SOFC anodes and may help to address sulfur-poisoning issues. This study has shown that sulfur incorporated in SOFC anodes during operation with sulfur-containing feed gases may exist in a whole variety of forms at post-test ambient conditions and can be distinguished well in the spectra. The comparison of the samples from the Real-SOFC project and from HEXIS indicates that the test history, in particular the cooling down might play an important role. Caution should be exercised when attempting to make conclusions about species formed during SOFC operation, when this is based on ambient temperature data only.

With more such experiments to come – we propose in situ studies at high temperature and controlled atmosphere, which are challenging but believed to be feasible, see Refs. [15,27] – we anticipate that the availability of sulfur-specific data will contribute to resolving the debate about what mechanisms of 'sulfur-poisoning' actually take place during SOFC operation.

Acknowledgements

Financial support by the European Union (Real-SOFC contract #SES6-CT-2003-502612, and contract MIRG-CT-2006-042095) and by the Swiss Competence Center for Energy and Mobility (CEMTEC project) are gratefully acknowledged. Part of the work was performed at the Swiss Light Source, Paul Scherrer Institut, Villigen, Switzerland. We are indebted to Wayne Stolte and Iraida N. Demchenko, University of Nevada Las Vegas and Advanced Light Source,

Lawrence Berkeley National Laboratory, Beamline 9.3.1, for support of this project.

References

[1] Fuel Cell Handbook, 7th ed. EG&G Technical Services, Inc. for NETL of U.S. Department of Energy, 2004.
[2] K. Sasaki, K. Susuki, A. Iyoshi, M. Uchimura, N. Imamura, H. Kusaba, Y. Teraoka, H. Fuchino, K. Tsujimoto, Y. Uchida, N. Jingo, J. Electrochem. Soc. 153 (11) (2006) A2023–A2029.
[3] J.R. Rostrup-Nielsen, J.B. Hansen, S. Helveg, N. Christiansen, A.-K. Jannasch, Appl. Phys. A 85 (2006) 427–430.
[4] Y. Matsuzaki, I. Yasuda, Solid-State Ionics 132 (2000) 261–269.
[5] M. Gong, X. Liu, J. Trembly, Chr. Johnson, J. Power Sources 168 (2007) 289–298.
[6] S. Chaturvedi, J.A. Rodriguez, J.L. Brito, Catal. Lett. 51 (1998) 85–93.
[7] J. Dong, Z. Cheng, Sh. Zha, M. Liu, J. Power Sources 156 (2006) 461–465.
[8] J.N. Andersen, Surf. Sci. 192 (1987) 583–596.
[9] A. Braun, H. Wang, S.S. Lee, E.J. Cairns, J.P. Shim, J. Power Sources 170 (2007) 173–178.
[10] A. Braun, H. Wang, U. Bergmann, M.C. Tucker, S.P. Weiwei Gu, E.J. Cramer, Cairns, J. Power Sources 112 (1) (2003) 231–235.
[11] O. Haas, U. Vogt, C. Soltmann, A. Braun, Xiao-Qing Yang, Won-Sub Yoon, T. Graule, The Fe K-edge X-Ray Absorption Characteristics of $La_{1-x}Sr_xFeO_{3-\delta}$. Prepared by Solid State Reaction, submitted to J. Solid State Chem. Ms. # JSSC-08-565.
[12] A. Braun, Carbon speciation in airborne particulate matter with C (1s) NEXAFS spectroscopy (critical review), J. Environ. Monit. 7 (11) (2005) 1059–1065.
[13] S. Pattanaik, F.E. Huggins, G.P. Huffman, W.P. Linak, C.A. Miller, Environ. Sci. Technol. 41 (2007) 1104–1110.
[14] G.P. Huffman, S. Mitra, F.E. Huggins, N. Shah, S. Vaidya, F. Lu, Energy Fuels 5 (1991) 574–581.
[15] H. Dathe, A. Jentys, J.A. Lercher, J. Phys. Chem. B 109 (2005) 21842–21846.
[16] H. Ota, T. Akai, H. Namita, Sh. Yamaguchi, M. Nomura, J. Power Sources 119–121 (2003) 567–571.
[17] S. Hay, J.B. Metson, M.M. Hylund, Ind. Eng. Chem. Res. 43 (2004) 1690–1700.
[18] M. Noponen, M. Halinen, J. Kiviaho, J. Saarinen, J. Fuel Cell Sci. Technol. 3 (4) (2006) 438–444.
[19] A.M. Flank, G. Cauchon, P. Lagarde, S. Bac, M. Janousch, R. Wetter, J.M. Dubuisson, M. Idir, F. Langlois, T. Moreno, D. Vantelon, Nucl. Instrum. Method B 246 (1) (2006) 269–274.
[20] D.W. Bishop, P.S. Thomas, A.S. Ray, Mater. Res. Bull. 35 (2000) 1123–1128.
[21] J. Cai, C. Raptis, Y.S. Raptis, E. Anastassakis, Phys. Rev. B 51 (1) (1995) 201–209.
[22] A. Wang, K.E. Kübler, B.L. Jolliff, L.A. Haskin, Am. Mineral. 89 (2004) 665–680.
[23] S. Music, M. Maljkovic, S. Popovic, R. Trojko, Croatia Chem. Acta 72 (4) (1999) 789–802.
[24] J. Stöhr, NEXAFS Spectroscopy; Springer Series in Surface Sciences 25, First Edition, Springer-Verlag, Berlin, Heidelberg, New York, 1992, ISBN 3-540-54422-4.
[25] A. Braun, S. Wirick, A. Kubátová, F.E. Huggins, G.P. Huffman, Atm. Environ. 40 (30) (2006) 5837–5844.
[26] A. Braun, A. Kubatova, S. Wirick, S.B. Mun, Radiation damage from EELS and NEXAFS in diesel soot and diesel soot extracts; Spec. Issue on Radiation Damages, J. Electron Spectros. Relat. Phenom. doi:10.1016/j.elspec.2007.08.002.
[27] M.M. Taghiei, F.E. Huggins, N. Shah, G.P. Huffman, Energy Fuels 6 (3) (1992) 293–300.
[28] A.J. Allen, A. Braun, C. Soltmann, J. Ilavsky, Anomalous ultra-small angle X-ray studies of solid oxide fuel cell assemblies at the Ni and Zr K-edges, in preparation.